Journal of Advanced Electrochemistry 2(2) (2016) 89–93

ISSN: 2455-0205

Contents List available at JACS Directory

Journal of Advanced Electrochemistry

journal homepage: http://www.jacsdirectory.com/jaec

Stress Corrosion Cracking of X-80 Pipeline Steel in Bioethanol

M. Rangel[1], J.G. Gonzalez-Rodriguez[1,*], S. Serna[1], A. Torres-Islas[2], B. Campillo[3]

[1]Universidad Autonoma del Estado de Morelos, CIICAp, Av. Universidad 1001, 62209 – Cuernavaca, Morelos, Mexico.
[2]Universidad Autonoma del Estado de Morelos, Fac. de Ciencias Quimicase Ing., Av. Universidad 1001, 62209 – Cuernavaca, Morelos, Mexico.
[3]Universidad Nacional Autonoma de Mexico, Fac. de Quimica, Mexico D.F.

ARTICLE DETAILS

Article history:
Received 28 Apr 2016
Accepted 14 May 2016
Available online 24 June 2016

Keywords:
Electrochemical Tests
Stress Corrosion Cracking
Bioethanol

ABSTRACT

A study on the susceptibility to stress corrosion cracking (SCC) of API X-80 pipeline steel in simulated fuel grade ethanol has been carried out by using slow atrain rate tests, polarization curves and noise in current measurements. Environmental factors included water (0, 1, 5, 10 and 20 vol.%) and chloride content (0, 10 and 32 g/L), whereas heat treatment included water quenched, quenched and tempered, oil quenched and water sprayed. Additionally some tests were carried out in absence of oxygen. Results have shown that X-80 carbon steel in the as-received condition was susceptible only when 5% water and 10 g/L of NaCl were present. Heat treatments suppressed this susceptibility. Conditions that increased the corrosion rate also increased the SCC susceptibility, which, together with metallographic observations and noise in current measurements, indicated that SCC in this environment is caused by a film rupture, dissolution mechanism.

1. Introduction

In order to reduce the amount of pollutants emitted in to the atmosphere and avoid the greenhouse effect, many counties, including Mexico, have started using biofuels, and for this reason, the use of ethanol in gasolina-ethanol blends has increased in the last few years [1]. The material used to transport gasoline-ethanol blends normally includes carbon steel which is very susceptible to stress corrosion cracking (SCC) in this environment [2] and a high number of accidents including this phenomenos have been reported, mainly in pipelines and storage gas tanks [3-5]. Many studies regarding this problem has been carried out using either commercial or simulated grade fuel ethanol (SFGE) [6-12] For instance, Beavers et al. [6] studied the effect of dissolved oxygen and inhibitors in different pipeline steel grades, welds, and heat affected zone on the susceptibility to SCC. They found that SCC did not occur even in ethanol-gasoline blends containing 15 vol. % ethanol, but SCC occur for ethanol contents either lower or higher than 15%. Deaerating the solution or water contents higher than 4.5 wt. % prevented from SCC to occur. Similarly, Lou et al. [7] evaluated the chloride, water and oxygen level on the SCC susceptibility of X-65 pipeline steel in SFGE. They found that chlorides affected greatly the SCC susceptibility, wherevers the water addition affected the steel passivation above 2.5%. In another study Sridhar et al. [3] carried out the effect of water, acetic acid, oxygen, corrosion inhibitor, chloride and methanol levels in SFGE on the SCC susceptibility on carbon steel. They found that galvanic coupling with precorroded steel increase the SCC susceptibility, whereas chloride had a less significant effect tan oxygen. In another work, Lou et al. [8] evaluated the SCC behaviour of X-65 carbon steel in SFGE by using SSRT, polarization curves, electrochemical impedance spectroscopy and potentiostatic tests. They concluded that crack initiation was associated with plastic deformation in the steel, which leads to surface film breakdown and the competition between anodic dissolution and repassivation at the crack tip determined the crack propagation. A similar conclusion was achieved by Goodman [9]. Samuzawa et al [10] evaluated the effect of acetic acid, formic acid, water contents (0.2, 1.0 and 4.0 vol. %) and chloride level (80 and 560 mg/L) on an X-52 carbon steel. They found that water, chloride and acetic acid level affects the pitting corrosion susceptibility, whereas formic acid promoted uniform type of corrosion. Thus, the goal of this work is to study the effect of water, chloride and oxygen level as well as heat treatment on the susceptibility to SCC of X-80 carbon steel in SFGE.

2. Experimental Methods

Material tested in this work includes an API X-80 carbon steel with chemical composition given in Table 1. In the as-received condition, slab samples measuring 1000 mm x 150 mm x 6750 mm were heated at 1200 °C, during 90 minutes and immediately hot rolled until achieving a final thickness of 25 mm at 820 °C. When the temperature reached 700 °C, slabs were cooled down to room temperature at a cooling rate 20 °C/h. Resulting microstructure was polygonal ferrite and 10% perlite. The yielding strength was 81,801 psi (564 M Pa), an UTS value of 83,963 psi (579 M Pa) and a percentage of elongation of 16%. Some heat treatments as indicated in Table 2 were carried out. Cylindrical tensile specimens with a 25.00 mm gauge length and 2.50 mm gauge diameter were machined. Before testing, the specimens were abraded longitudinally with 600-grade emery paper, degreased, and masked, with the exception of the gauge length. Specimens were subjected to conventional, monotonic slow strain rate tensile (SSRT) testing in dry air as an inert environment, and in SFGE with a composition as given in Table 3. The loss in ductility was assessed in terms of the percentage reduction in area (%*R.A*) by using:

$$\%R.A. = \frac{A_i - A_f}{A_i} x100 \qquad (1)$$

where A_i and A_f are the initial and final area respectively. Tensile-fractured specimens were examined by a JEOL scanning electron microscope (SEM). Changes in the water contents were carried out by using distilled water. Additionally, some tests were performed by changing the chloride contents, i.e. 0, 10 and 32 mg/L, in deareted conditions, and under different heat treatment conditions as given in Table 2. Potentiodynamic polarization curves were carried out in a conventional three electrode electrochemical cell from -800 up to + 600 mV with respect the free corrosion potential value, E_{corr}, at a scan rate of 1 mV/s (60 mV/min), using a graphite rode and a saturated calomel electrode (SCE) as auxiliary and reference electrodes respectively. Working electrodes were cylindrical pieces having 6 mm in diameter encapsulated in commercial epoxy resin. Corrosion current values, I_{corr}, were calculated by using the Tafel extrapolation method. Some electrochemical noise (EN) measurements during the SSRT experiments were made recording the current

---

*Corresponding Author
Email Address: ggonzalez@uaem.mx (J.G. Gonzalez-Rodriguez)

Cite this Article as: M. Rangel, J.G. Gonzalez-Rodriguez, S. Serna, A. Torres-Islas, B. Campillo, Stress Corrosion Cracking of X-80 Pipeline Steel in Bioethanol, J. Adv. Electrochem. 2(2) (2016) 89–93.

fluctuations at a sampling rate of 1 point per second in blocks of 1024 readings. EN readings were taken every hour during the whole straining test. A fully automated zero resistance ammeter (ZRA) from ACM instruments was used in this case.

Table 1 Chemical composition of API X-80 pipeline steel (wt. %)

C	Si	Mn	P	S	Cr	Mo	Ni
0.0393	0.1160	1.470	0.0125	0.0044	0.2387	0.0352	0.1426
Al	Co	Cu	Nb	Ti	V	Pb	Fe
0.0835	0.0037	0.2763	0.0860	0.0111	<0.0000	0.0053	97.5

Table 2 Heat treatments given to X-80 steel.

Heat treatment	Conditions
Water quenched	850 °C, 40 minutes, quenched in static water
Water quenched and tempered	850 °C, 40 minutes, quenched in static water, heated at 400 °C during 20 minutes
Water sprayed	850 °C, 40 minutes, cooled in sprayed water
Oil quenched	850 °C, 40 minutes, quenched in static oil

Table 3 Chemical composition of base SFGE solution.

Water (vol.%)	Metanol (vol.%)	Acetic acid (mg/L)	NaCl (mg/L)	Ethanol
1	0.5	56	10	balance

3. Results and Discussion

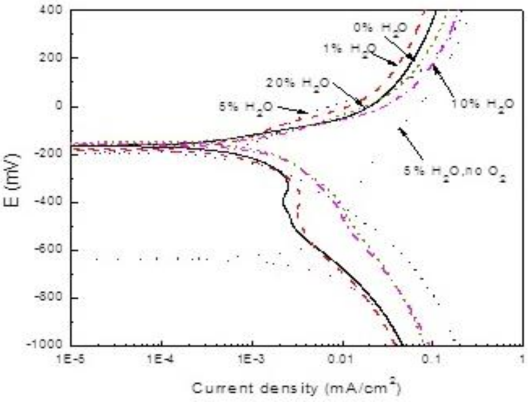

Fig. 1 Effect of SFGE water and oxygen contents in the polarization curves for X-80 carbon steel

The effect of water contents in the polarization curves for the as-received X-80 carbon steel in SFGE is given in Fig. 1. For comparison, the polarizatin curve in absence of oxygen is also given. In prescence of oxygen, it can be seen that, in the anodic branch of the curve, anodic current density increases with the apllied potential without evidence of a passivation except for water contents of 1 and 5%, which has been atributed to the prescence of relatively stable Surface alcoxy (methoxy and/or ethoxy) compounds such as pseudo-passivating $Fe\text{-}OCH_3$ [14-16]. The pitting potential value, Epit, was higher for the solution containing 5% H_2O than that containing 1% H_2O.The Ecorr value practically was unaffected by the water contents, but the Icorr value was, increasing with increasing the water contents, reaching a maximum value with 5% H_2O, and decreased with a further increase in the H_2O contents. The anodic current density increased with the water contents, reaching its highest value with a water contents of 5%, and then it decreased with a further increase in the water contents. Samuzawa et al. [9] found a passive region for X-52 carbon steel in a very similar SFGE solution, being the only difference tha chloride contents, i.e. 8 mg/L. However, they also found that by increasing the water contents from 0.2 to 4.0 vol.% the anodic current density increased, but the susceptibility to pitting type of corrosion decreased. When oxygen was removed form solution, the Ecorr value shifted in to a more active regi0n, the Icorr and anodic current density values increased, and there was a passive region with a pitting potential value around -250 mV. Similar results were found for X-65 carbon steel in SFGE solution [5]. Thus, the prescence of oxygen increased the uniform corrosion and decreased the pitting potential value, increasing, thus, the susceptibility towards pitting type of corrosion.

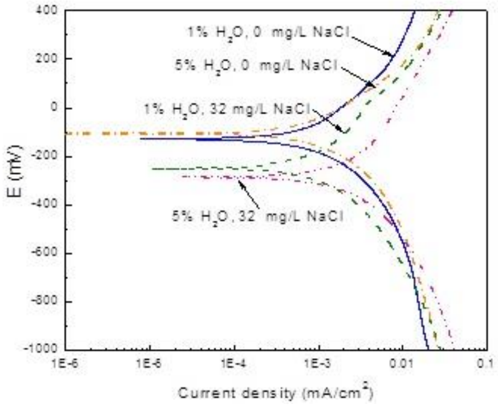

Fig. 2 Effect of SFGE water and NaCl contents in the polarization curves for X-80 carbon steel

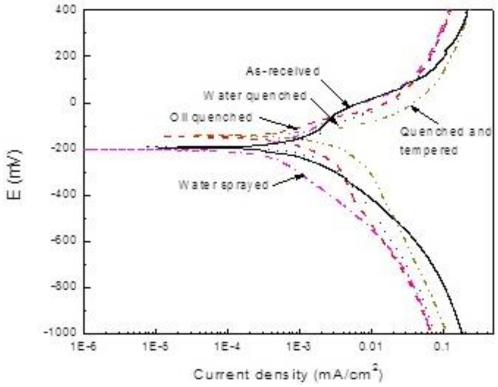

Fig. 3 Effect of heat treatment in the polarization curves for X-80 carbon steel in SFGE

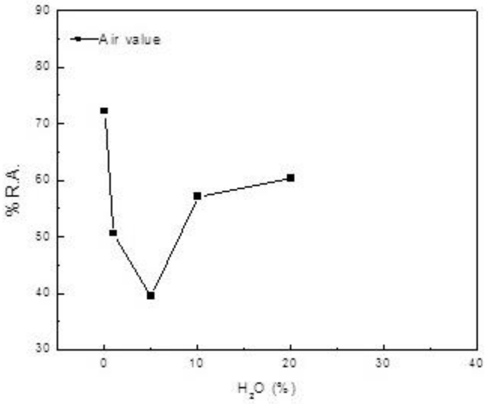

Fig. 4 Effect of SFGE water contents in the % R.A. value for X-80 carbon steel

The effect of both chloride and water contents in the polarization curves for the as received X-80 steel in SFGE solution is shown in Fig. 2, were it is clear that, in all cases, the anodic current density and the I_{corr} values increased by increasing the water and chloride levels. In addition to this, the presence of chloride in the 1% H_2O solution induced a passive region, and thus, the pitting susceptibility increased. The prescence of a passive region in the solution containing 5% water was not so obvious, only an increase in the uniform corrosion rate was observed. Finally, the effect of heat treatment in the polarization curves in SFGE is shown in Fig. 3, where it can be seen that the E_{corr} value remained more or less unaltered, but the I_{corr} value was decreased for the oil quenched and the water sprayed heat treatments, whereas an increase was observed for the water quenched and in the quenched and tempered conditions. All the conditions exhibited an active-passive behaviour, with the widest passive zone and the highest E_{pit} value was for the steel in the as-received condition, whereas the lowest pitting potential value was for the steel in the water quenched and tempered condition.

The effect of water contents in SFGE on the percentage reduction in area % R.A. for the as-received X-80 carbon steel is given in Fig. 4. This figure shows that the % R. A. decreases as the water contents increases from 0 to 5%, reaching its lowest value at 5% H_2O, but the steel recovers its ductility with a further increase in the water contents higher than 5%, although the highest % R.A. was 65 for a water contents of 20%, so the ductility recovery was not complete since the % R.A. obtained in air was 85, and that value for a water contents of 5% was only 40%. Lou [5] working with X-65 carbon steel in SFGE solution found that 1% water was enough to cause SCC, whereas 2% H_2O, pitting corrosion was reported which changed to general corrosion at 5% or higher water content. No SCC was observed in SSRT of pipeline steels in SFGE containing 5 vol. % H_2O. This is so because high corrosion rates and unstable passive film formation, leading to a general attack and crack blunting.

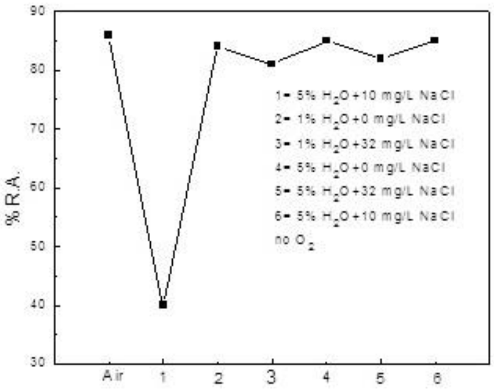

Fig. 5 Effect of SFGE water, NACl and oxygen contents in the % R.A. value for X-80 carbon steel

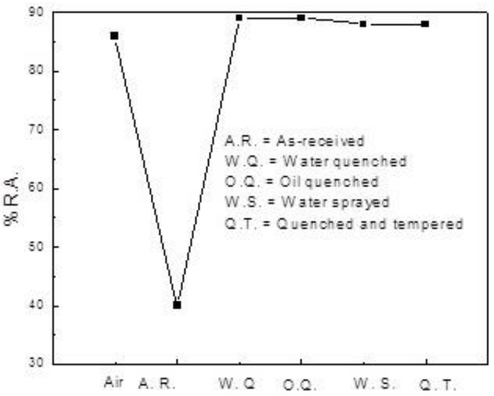

Fig. 6 Effect of heat treatment in the % R.A. value for X-80 carbon steel in SFGE

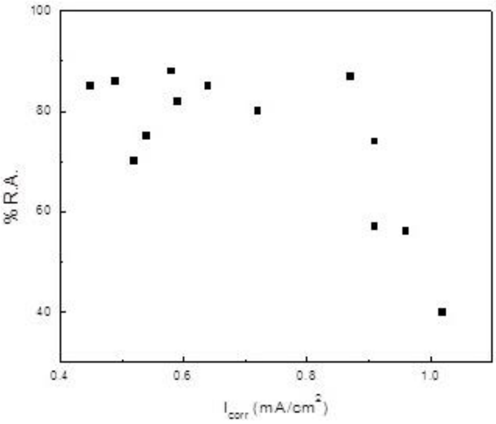

Fig. 7 Effect of the I_{corr} in the % R.A. value for X-80 carbon Steel in SFGE in all the tested condition

When the effect of chloride level on the % R.A. value was studied, Fig. 5 we can see that neither removing the chloride level nor increasing it to 32 mg/L in the SFGE containing 5% water increased the SCC susceptibility. Similarly, in the SFGE containing 1% water, neither eliminating the chloride level nor increasing it to 32 mg/L made the X-80 carbon steel susceptible to SCC. Thus, as we have seen from the polarization curves, Fig. 2, the increment in either the water or chloride level in SFGE increased the SCC susceptibility for X-80 carbon steel, only increased the general corrosion rate. Similarly, the re-motion of oxygen on the SFGE base solution did not make the steel more susceptible to SCC since its % R.A. value was very similar to that value obtained in air, 85%. Thus, the absence of oxygen in SFGE increased the uniform corrosion rate for X-80 carbon steel, Fig. 1 but not its SCC susceptibility as reported elsewhere [5,6]. This is so because high dissolution rates leads to unstable passive film formation and crack tip blunting [5, 6]. Something very similar was observed when the effect of the heat treatment in the % R.A. value for X-80 carbon steel in the base SFGE solution was studied, Fig. 6. We can see that none of the heat treatments, even the quenched conditions, increased the SCC susceptibility and only in the as-received condition the steel was susceptible to SCC.

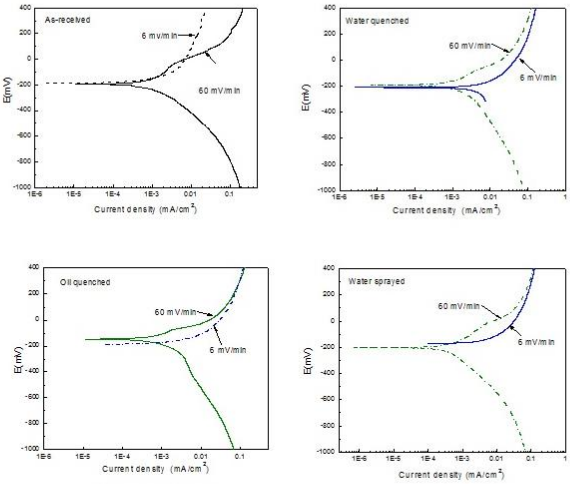

Fig. 8 Effect of the sweep rate in the polarization curves for X-80 carbon steel in SFGE under the different heat treatments given

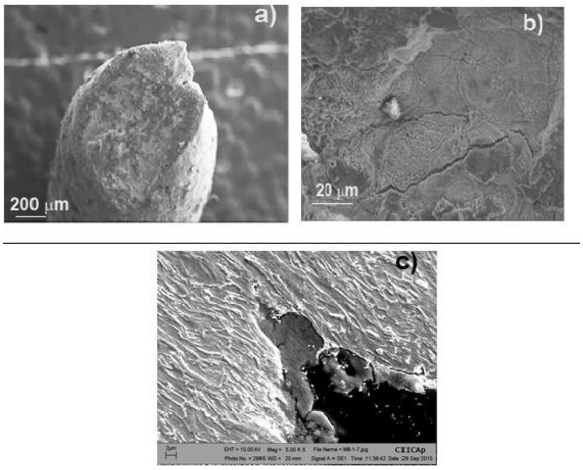

Fig. 9 SEM micrograph of X-80 carbon steel fractured in SFGE containing 5% H_2O + 10 mg/L NaCl showing in a) top view, b) and c) transgranular crack with corrosión products

Corrosion rates, in terms of corrosion current density values, were obtained from polarization curves in all the tested conditions, and Fig. 7 shows the effect of the Icorr value in the % R. A. results for all tests. From this figure it is clear that an increase in the corrosion rate leads to a reduction in the steel ductility as measured in the % R.A. which led us to think that the anodic dissolution mechanism is the responsible for the SCC susceptibility for X-80 carbon steel in SFGE solution. The tendency of the steel to fail by SCC caused by film rupture was evaluated on the basis that there was at least one order of magnitude difference in the passive current density value, Ipas between the slow and fast sweeps [17, 18]. To test this, some polarization curves but at a lower sweep rate, 6 mV/min, ten times slower than the normally used in this work, 60 mV/min. Polarization curves at the 2 sweep rates for X-80 carbon steel in the different heat treatment condition is shown in Fig.8. Using this criteria, we can see that the only the steel in the as-received condition made X-80 carbon steel more susceptible to SCC, since in this condition the difference in the Ipas value between the fast and slow sweeps was one order of magnitude. Fractographic analysis of the as-received X-80 carbon Steel fractured in the SFGE solution containing 5% H_2O, Fig.9, shows the trans granular mode of cracking of this specimen, and the presence of corrosion products inside the crack, which is an evidence that the SCC of X-80 carbon steel in this solution occurred by the dissolution process of metal at the crack tip as found in [19] but for X-65 carbon steel in carbonate/bicarbonate solutions.

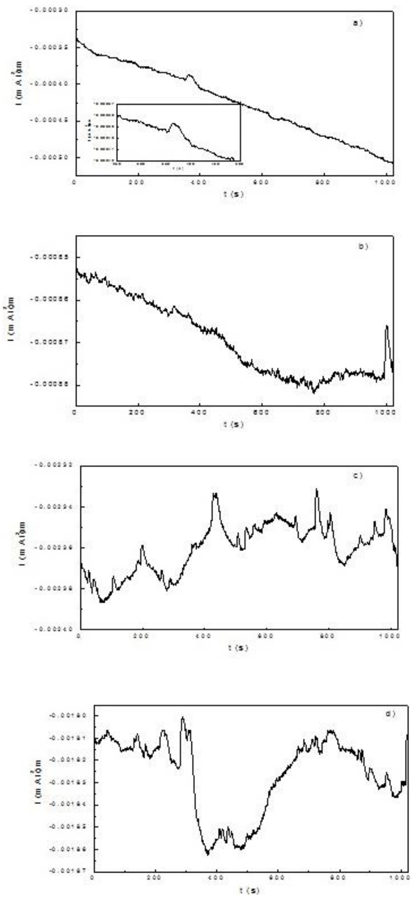

Fig. 10 Time series in current for strained X-80 carbon steel fractured in SFGE containing 5% H_2O + 10 mg/L NaCl taken at a) beginnig of straining, b) yielding point, c) near the UTS value and d) after the UTS, before final fracture

Since SCC has been proved to be greatly influenced by the corrosion performance and the repassivation kinetics of a bare or unfirmed steel [20, 21] and in order to test that X-80 carbon steel was susceptible to SCC in SFGE by a film rupture mechanism, some electrochemical noise in current during the SSRT for the steel fractured in the SFGE solution containing 5% H_2O were carried out, and the results are given in Fig. 10. This figure shows the noise in current readings at the beginning of the straining, at the yielding point, at the UTS value and just before final fracture. At the beginning of the straining time series consists of transients with high frequency and low intensity, lower than 1 X10^{-5} mA/cm^2, which are due to the rupture of the passive layed by this straining and its rapid repassivation. At the yielding point, the noise transients showed a sudden increase in its intensity and a slow recovery, they increased its intensity, lower than 1 x10^{-4} mA/cm^2, which are still due to the rupture of the passive layer by straining and its rapid repassivation. At these two points, transients showed a frequency which is more or less constant. However, after the yielding point, Fig.10 c, the frequency of the noise transients decreased and the intensity increased, reaching values of 1 x 10^{-3} mA/cm^2 which are believed to be due to a rupture of the passive layer and its repassivation but inside the crack [22-29]. Bidhar [22] working with 316 type stainless steel in high purity oxygenated water at 288 degrees, found spike-like current transients after the yielding point and correlated this fact with a slip dissolution processes. In a similar way, Stewart [23] working with 316 type stainless steel in high purity oxygenated water at 288 degrees found current pulses associated with the nucleation of micro cracks and their movement across single grain boundaries during the inter granular SCC of this steel and associated them to the crack-tip dissolution. Kovac et al [27] when studying the SCC behaviour of 304 stainless steel in sodium thiosulphate solution, also found that when cracking started, the current noise showed an increase in intensity but towards the final fracture some smaller sharp transients of EN current were observed. Thus, all the evidence indicates that the cracking process occurs through a film rupture, anodic dissolution process. The repassivation and corrosion behaviour in a crack tip depends on some environmental parameters which will affect its SCC susceptibility: if the corrosion rate and thus film growth rate is too high, there will be no crack propagation; on the other hand, if corrosion rate is too low, a crack would not maintain its geometry and would blunt in favor of general corrosion [30].

It has been proven that, even under conditions that favor anodic dissolution, electrochemical conditions inside a pit or a crack are such that hydrogen discharge is possible. Parkins, working with X-65 carbon steel in an NS-4 solution containing diluted carbon dioxide (CO_2), considered that the results suggested dissolution and hydrogen ingress into the steel [19]. Similar results were found by Gu et a. [31] for X-80 steel in the same solution. However, in the NS-4 solution, X-80 steel did not show a passive region, whereas in this study it did, Fig. 1, demonstrating the importance of the film rupture. The presence of corrosion products and the current transients during the SSRT experiments are an evidence of the importance of the dissolution and repassivation at the crack tip, where the rupture of the passive film inside the crack led to a rapid dissolution at the crack tip, whereas the crack walls remains in the passive state [18]. Similar conclusions were achieved in some other works for pipeline steels in SFGE solutions [4-8, 13-18, 32]. Indicating that SCC in this environment is caused by a film rupture, dissolution mechanism, dissolution of the steel at the bare crack tip, and a propagation of the crack into the bulk material. Strain induced deformation exposes fresh metal at the crack tip. Unprotected bare metal at the crack tip, which is connected to the passivated crack walls in oxygenated ethanol shifts these zones towards an anodic direction, and thus, to allow the crack tip advance by dissolution.

4. Conclusion

X-80 carbon steel was susceptible to SCC only in a normally aerated SFGE solution containing 5 vol. % H_2O+10 g/L NaCl. Either lower or higher amounts of H_2O did not induce SCC. Additionally, neither increasing nor decreasing the NaCl level present in the solution made X-80 carbon steel susceptible to SCC. By eliminating oxygen dissolved in the SFGE solution increased the corrosion rate but not the SCC susceptibility. Given a heat treatment such as water quenched, quenched and tempered, oil quenched or water sprayed suppressed the SCC susceptibility for X-80 carbon steel. Metallographic evidence and noise in current measurements showed that SCC in this environment is caused by a film rupture, dissolution mechanism.

References

[1] A. Demirbas, Yields of oil products from thermochemical biomass conversion processes, Energy Convers. Manage. 49 (2008) 2106-2114.

[2] R.D. Kane, D. Eden, N. Sridhar, J. Maldonado, A.K. Agarwal, J.A. Beavers, M.P.H. Brongers, Stress corrosion cracking of carbon steel in fuel-grade ethanol: Review, experience survey, field monitoring, and laboratory testing, API Technical Report 939-D, American Petroleum Institute, Washington, D.C., 2007.

[3] N. Sridhar, K. Price, J. Buckingham, J. Dante, Stress corrosion cracking of carbon steel in ethanol, Corrosion 62(3) (2006) 687-702.

[4] R.D. Kane, N. Sridhar, M.P.H. Brongers, J.A. Beavers, A.K. Agrawal, L.J. Klein, Stress corrosion cracking in fuel ethanol: A recently recognized phenomenon, Mater. Perform. 44(1) (2005) 50-59.

[5] X.Y. Lou, D. Yang, P.M. Singh, Effect of ethanol chemistry on stress corrosion cracking of carbon steel in fuel-grade ethanol, Corrosion 65(6) (2009) 785-797.

[6] J.A. beavers, F. Gui, N. Srighar, Effects of environmental and metallurgical factors in the stress corrosion cracking of carbon steels in fuel-grade ethanol, Corrosion 67(3) (2011) 025005-1.025005-15.

[7] X. Lou, D. Yang, P.M. Singh, Film breakdown and anodic dissolution during stress corrosion cracking of carbon steel in bioethanol, J. Electrochem. Soc. 15 (2010) 86-94.

[8] L.R. Goodman, P.M. Singh, Repassivation behaviour of X65 pipeline steel in fuel grade ethanol and its implications for the stress corrosion cracking mechanism, Corros. Sci. 65(1) (2012) 238-248.

[9] I. Samusawa, K. Shiotani, Influence and role of ethanol minor constituents of fuel grade ethanol on corrosion behaviour of carbon steel, Corros. Sci. 90(1) (2015) 266-275.

[10] X. Lou, P.M. Singh, Phase angle analysis for stress corrosion cracking of carbon steel in fuel-grade ethanol: Experiments and simulation, Electrochem. Acta. 56(9) (2011) 1835-1847.

[11] J. Torkkeli, T. Saukkonen, H. Hänninen, Effect of MnS inclusion dissolution on carbon steel stress corrosion cracking in fuel-grade ethanol, Corros. Sci. 96(1) (2015) 14-22.

[12] L. Cao, G.S. Frankel, N. Sridhar, Effect of oxygen on ethanol stress corrosion cracking susceptibility: Part 2-Dissolution-based cracking mechanism, Corrosion 69(7) (2013) 851-862.

[13] J.W. Sowards, T.S. Weeks, J.D. McColskey, The influence of simulated fuel-grade ethanol on fatigue crack propagation in pipeline and storage-tank steels, Corros. Sci. 75(4) (2013) 415-425.

[14] J. Banaś, B. Stypuła, K. Banaś, J. Światowska-Mrowiecka, M. Starowicz, U. Lelek-Borkowska, Corrosion and passivity of metals in methanol solutions of electrolytes, J. Solid State Electrochem. 13(9) (2009)1669-1679.

[15] Ch. Sendner, S. Sakong, A. Grob, Kinetic montoring carlo simulations of the partial oxidation of methanol on oxygen-covered Cu (1 1 0), Appl. Surf. Sci. 60(9) (2006) 3258-3265.

[16] H.E. Anders, P. Gardnem, D.A. King, Absence of dielectric relaxation effects on intramolecular electron transfer in porphyrin-quinone cyclophanes, Chem Phys. Lett. 231 (1994) 481-485.
[17] J.M. Sutcliffe, R.R. Fessler, W.K. Boyd, R.N. Parkins, Stress corrosion cracking of carbon steel in carbonate solutions, Corrosion 28(3) (1972) 313-320.
[18] R.N. Parkins, The controlling parameters in stress corrosión cracking, 5th Symp. On Line pipe Research, Paper no. L30174, Arlington, VA, AGA, 1974, p. 324.
[19] R.N. Parkins, Mechanistic aspects of intergranular stress corrosion cracking of ferritic steels, Corrosion 52(3) (1996) 363-374.
[20] J.C. Scully, Kinetic features of stress corrosion cracking, Corros. Sci. 7(2) (1967) 197-207.
[21] J.C. Scully, Stress corrosion crack propagation: a constant charge criterion, Corros. Sci. 15(2) (1975) 207-224.
[22] S.K. Bidhar, Y. Watanabe, H. Tsukui, T. Uchimito, Understanding and detecting early stages of SCC initiation in sensitized stainless steel by means of electrochemical potential transient, Prog. Fract. Str. Mater. Struct. 353 (2007) 2387-2394.
[23] J. Stewart, D.B. Wells, P.M. Scott, Electrochemical noise measurements of stress corrosion cracking of sensitised austenitic stainless steel in high-purity oxygenated water at 288 °C, Corros. Sci. 33(1) (1992) 73-88.
[24] M.G. Pujar, N. Parvathavarthini, R.K. Dayal, S. Thirunavukkarasu, Assessment of intergranular corrosion (IGC) in 316(N) stainless steel using electrochemical noise (EN) technique, Corros. Sci. 51(9) (2009) 1707-1713.
[25] G.L. Edgemon, M.J. Danielson, G.E.C. Bell, Detection of stress corrosion cracking and general corrosion of mild steel in simulated defense nuclear waste solutions using electrochemical noise analysis, J. Nuclear Mater. 245 (1997) 201-209.
[26] J. Hickling, D.F. Taylor, P.L. Andresen, Use of electrochemical noise to detect stress corrosion crack initiation in simulated BWR environments, Mater. Corros. 49(5) (1998) 651-658.
[27] J. Kovac, M. Leban, A. Legat, Detection of SCC on prestressing steel wire by the simultaneous use of electrochemical noise and acoustic emission measurements, Electrochem. Acta 52(12) (2007) 7607-7616.
[28] T. Anita, M.G. Pujar, H. Shaikh, R.K. Dayal, H.S. Khatak, Assessment of stress corrosion crack initiation and propagation in AISI type 316 stainless steel by electrochemical noise technique, Corros. Sci. 48(8) (2006) 2689-2710.
[29] G. Du, J. Li, W.K. Wang, C. Jiang, S.Z. Song, Detection and characterization of stress-corrosion cracking on 304 stainless steel by electrochemical noise and acoustic emission techniques, Corros. Sci. 53(9) (2011) 2918-2926.
[30] J.S.L. Leach, The possible role of surface films in stress corrosion cracking, R.W. Stahele (Ed.), Stress corrosion cracking and hydrogen embrittlement of iron base alloys, NACE International, Houston, Texas, 1977.
[31] B. Gu, W.Z. Liu, J.L. Luo, X. Mao, Trans granular stress corrosion cracking of X-80 and X-52 pipeline steels in dilute aqueous solution with near-neutral pH, Corrosion 55(3) (1999) 312-318.
[32] R.C. Newman, Review and hypothesis for the stress corrosion mechanism of carbon steel in alcohols, Corrosion 64(7) (2008) 819-823.

Cite this Article as: M. Rangel, J.G. Gonzalez-Rodriguez, S. Serna, A. Torres-Islas, B. Campillo, Stress corrosion cracking of X-80 pipeline steel in bioethanol, J. Adv. Electrochem. 2(2) (2016) 89–93.